Stability and properties of the cluster assembled solid phases of X_8C_{12} and YX_7C_{12}

2005 J. Phys.: Condens. Matter 17 2571

(http://iopscience.iop.org/0953-8984/17/17/005)

INSTITUTE OF PHYSICS PUBLISHING JOURNAL OF PHYSICS: CONDENSED MATTER

J. Phys.: Condens. Matter **17** (2005) 2571–2584 doi:10.1088/0953-8984/17/17/005

Stability and properties of the cluster assembled solid phases of X_8C_{12} and YX_7C_{12}

H S Domingos

Department of Materials Science and Metallurgy, University of Cambridge, Pembroke street, Cambridge CB2 3QZ, UK

Received 4 November 2004, in final form 1 March 2005
Published 15 April 2005
Online at stacks.iop.org/JPhysCM/17/2571

Abstract

We have investigated several of the most stable cluster assembled phases of X_8C_{12} and YX_7C_{12} (X, Y = B, N, Si) using pseudopotential plane-wave density functional theory. We have found that many of these were stable, conductive and retained the integrity of the cluster cage, along with some of its bonding characteristics. A large range of metastable molecular solids can be produced in this way. Some of these new covalent conductors and one semiconductor were considered good candidates for high T_c superconductivity and may constitute an improvement over the recently discovered fcc-C_{22} superconducting molecular solid.

1. Introduction

The discovery of the Ti_8C_{12} transition metal carbide cluster of special stability by Castleman and co-workers [1, 2] has shown the existence of the metallocarbohedrenes (Met-Cars), a new and unexpected class of clusters with still poorly understood properties. Met-Cars may be related to the dodecahedral C_{20}, which is the smallest fullerene. C_{20} was expected to be metastable due to the high strain of the bonds of its highly curved sp^2 coordinated surface. Prinzbach *et al* [3] have succeeded in producing it starting from the saturated hydrocarbon dodecahedrene $C_{20}H_{20}$ [3]. C_{20} and derived Met-Car related structures have been the subject of theoretical [4–8] and experimental [9] studies, which confirm that its extreme curvature enhances the reactivity of its carbon cage and makes it an ideal candidate for assembly into one, two and three-dimensional structures. A metallic, covalently bonded, carbon-based solid with a high degree of crystallinity is necessary to obtain large electron–phonon coupling and one of these C_{20} based structures has already been synthesized [9–11]. These conditions can be taken as prerequisites for high T_c superconductivity and it has been proposed that solid phases assembled from C_{20} (fcc-C_{22}) will be high T_c superconductors [10–16] with transition temperatures of up to 55 K. It is then important to find out which phases are metastable and what some of their properties may be, not just to access the superconductive characteristics, and aid design, but also to be able to recognize the structures once they are synthesized.

The stability of some X_8Y_{12}, X_8C_{12} and YX_7C_{12} (X, Y = B, N, Si) Met-Car analogue clusters has been investigated. It has been proposed that there are solid phases assembled from

them with high T_c superconducting properties [12]. Many isomers are possible for the isolated clusters and recent research has aimed at determining which ones are the most stable and what their properties might be [4–7].

In this work we compare the stability of solid structures of different symmetries resulting from the assembly of the isolated Met-Car analogue clusters C_{20}, B_8C_{12}, B_8N_{12}, N_8B_{12}, N_8C_{12}, Si_8C_{12} and the three-species analogue clusters SiB_7C_{12}, SiN_7C_{12} and BN_7C_{12}. We subsequently investigate the feasibility of assembling the clusters into lattices that are simple cubic, body- and face-centred cubic, orthorhombic and triclinic. Our aim is to identify not only which of these solids are the most stable but also the ones that are metallic and assess their potential for high T_c superconductivity by evaluating the characteristics of the various phases. The general aim is also to prove the wide variety of solids that can result from such assemblies. While it is impossible to exhaust all structures for each cluster and solid, we have studied those that are the most probable according to the available experimental and theoretical data for compounds of this type. The clusters are known to be electronegative, their $-1/-2$ charge states are energetically favoured [8] and the clusters tend to be highly reactive. Relevant to our study is the finding that the assembly of zirconium Met-Cars in stable solids does take place under soft landing conditions [17], oligomers are expected to be stable [8, 18] and for several of the clusters we found different phases of comparable stability. Important questions are whether several of these stable phases can coexist, and if in this case superconductive behaviour can occur in different allotropes. Many different polymers could be fabricated, aiming toward the design of novel classes of conductors, semiconductors and high T_c superconductors. Polymerized linear chains of clusters and their possible inclusion in nanotubes and zeolites are suggested but not explored.

We have chosen the clusters involving B, N and Si for several reasons. (a) They form organic or organometallic clusters with a variable number of π bonds. (b) The intra-cluster bonding is guaranteed to be strong. (c) C_48X_{12} with the same elements has been observed [19]. (d) The clusters are likely to assemble solids.

The restrictions that we have imposed on the search for solids has been twofold. First, we have demanded that the isomers have a T_h symmetry skeleton, since this has been considered the most probable configuration. Second, we have only considered the most probable spacial arrangements for the clusters and not all possible structures. This is justified by the work on C_{20} based solids, where the fcc, sc and orc phases were the main candidates for assembly and fcc is the one that is experimentally observed.

2. Computational method

We performed density functional calculations within the spin independent generalized gradient approximation (GGA) for exchange and correlation as parametrized by Perdew and Wang [20]. All calculations were carried out with the CASTEP [21] program using a plane-wave basis set. The pseudopotentials were of the ultra-soft type [22] and included s and p projectors. Periodic boundary conditions were used in all the calculations but no symmetry constraints were applied in the optimization of atomic coordinates or unit cells. The supercell approximation was used for calculations on isolated clusters, whereby a separation of at least 15 Å between a cluster and its mirror images ensured that the interactions between them were kept to a negligible level. The kinetic energy cut-off was selected so that energies were converged to less than 0.01 eV/atom. The convergence thresholds for atomic relaxation were 0.05 eV $Å^{-1}$/atom for the forces and 2×10^{-5} eV for the total energy. Our k-point sampling mesh [23] for a unit cell with 20, 88, 48 or 1 atoms had a density of 0.06 $Å^{-1}$ and included the Γ point. The binding energies were calculated with respect to the free atoms, first within the generalized gradient

approximation (GGA) and then within the generalized gradient spin-density approximation (GGS). The isolated atoms were calculated in a $10 \times 10 \times 10$ Å^3 box. The Mulliken, overlap populations (BO) and partial density of states (PDOS) were calculated by projecting the valence charge onto pseudoatomic wavefunctions [24]. The spilling parameter was in every case inferior to 2.5%. The Gaussian smearing used for the density of states (DOS) was 0.2.

The difference between GGA and GGS total energies for the clusters was confirmed to be small and did not depend significantly on the open or closed-shell structures and so the stability considerations do not have to rely on spin-dependent calculations. The stabilization energies were calculated as the difference between the cluster in isolation and the cluster in the bulk solid. The binding energies for the clusters were defined as the total energy minus the isolated atoms divided by the number of atoms in the cluster. The stabilization energies with respect to solids and other structures were defined as the difference between binding/cohesive energies for the structures multiplied by the number of atoms in one cluster (20). The isolated atoms were calculated within GGA and GGS. Again the GGA versus GGS values for the solids did not differ significantly in proportion to the absolute values (≈3% between the total energy of the clusters and 0.15% between the atomization energies).

We have used the nomenclature C_{20} (T_h) fcc for the solid fcc-C_{22} [9], since it is more explicit in our context. In the same way C_{20} (T_h) bcc refers to a hypothetical structure of bcc-C_{24}. The assembly is of C_{20} clusters linked by four (twofold coordinated) interstitial carbon atoms per cluster. The same nomenclature is adopted for mixed element clusters.

3. Energetics

We have found that the B_8C_{12} clusters can form at least five metastable phases (see figure 1).

(a) A simple cubic lattice (sc) with open cage structure and C=C ethylenic inter-cluster bonding.
(b) A closed cage structure and C–C inter-cluster bonding.
(c) A body centred orthorhombic (bcc) phase with C–C bonding and closed T_h cage.
(d) A face centred phase (fcc) with two interstitial fourfold coordinated carbon atoms per cluster, which is not stable for B_8C_{12}.
(e) An sc (C_{2v}) closed cage structure and
(f) an orthorhombic (orc) phase where the cluster is absent, but which is related by Stone–Wales transformations.

There was an sc derived phase, which we have called trc, which is the initial sc structure with B–C bonds. This then relaxed through bond relaxation to a triclinic (trc) unit cell. The stabilization (eV/cluster) and cohesive energies (eV/atom) are shown in table 1. The simple cubic lattice with C=C inter-cluster bonding (a) is the most stable, followed by the simple cubic-like B–C inter-cluster bonded one, which relaxed to a trc structure through bond distortion. There was no transition barrier for the most stable phase, where the structure was relaxed from a closed cage (sc) configuration. We predict that phase (a) is the most probable, since it is highly stable and it can result from direct cluster assembly, in contrast to C_{20}, where fcc ($Fm\bar{3}$) is the most stable [11]. B_8C_{12} (T_h) clusters tend to stabilize in an sc ($Pm\bar{3}$) structure [12]. This phase is metallic and its stabilization energy is considerably larger than any of the others. Nevertheless, all of the other calculated phases are metallic and, like sc, show a high degree of crystallinity. Table 1 shows the binding energies (BE) calculated as atomization or cohesive energies using both the GGA and GGS values for the isolated atom energies. The stabilization energies (SE) per cluster (20 atoms) are also shown, with the values obtained from GGA atoms. The type of lattice and the space group symmetries for each polymerized structure are indicated.

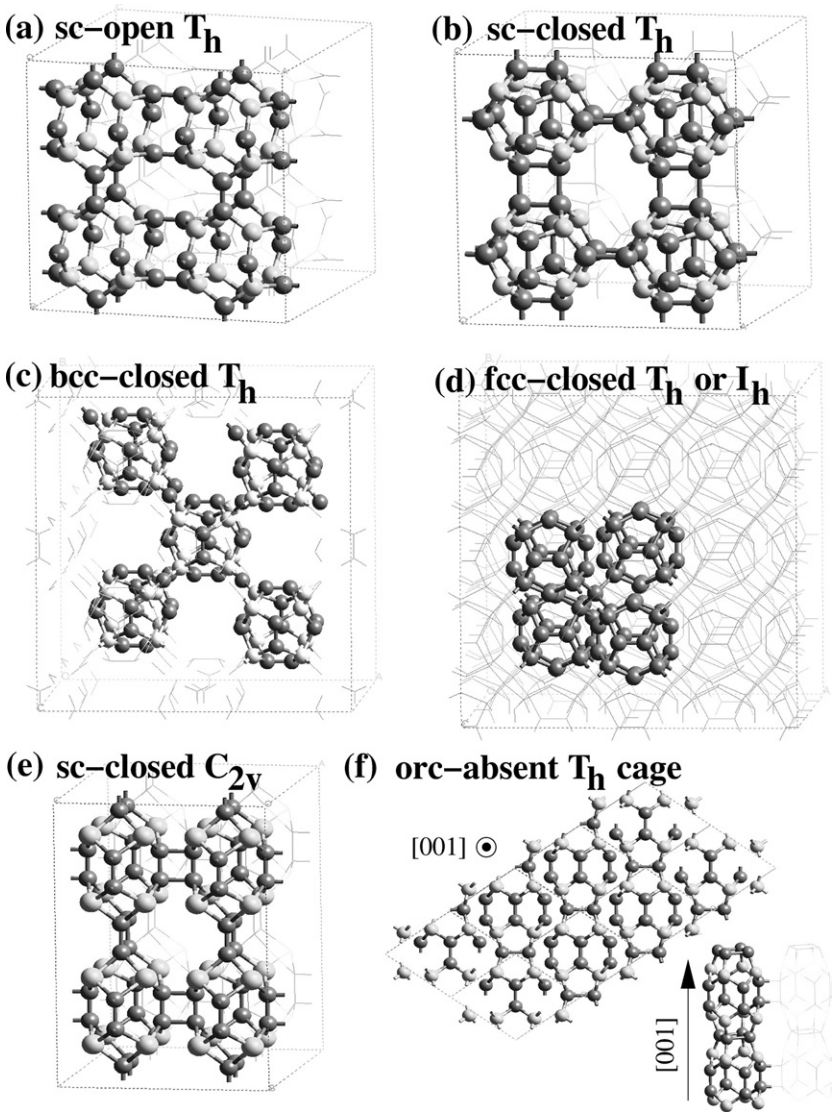

Figure 1. The geometries for the cluster assembled phases are depicted. (a) Simple cubic sc, T_h point symmetry open cage structure. (b) The closed cage sc configuration. (c) The bcc structure with twofold bonded carbon interstitials. (d) The fcc structure (fcc-C_{22}) with two sp^3 bonded carbon interstitials per cluster. If the cluster is C_{20} the cluster symmetry is I_h and if it is another of the clusters that we have considered it is T_h, both in a closed cage configuration. (e) The sc closed C_{2v} cluster solid and (f) the orc phase, where the cluster is absent. At the bottom right we can see the repeating chain that is part of the structure. There are at least three other metastable structures that can be derived from this one but none of them is energetically competitive with the sc open cage, nor can they result from plain cluster assembly.

The BE(GGS) values are expected to be a better approximation to the experimental cohesive energies but these do not alter the stabilization energies.

Three solids for the C_{20} assembly were calculated and reported in previous work [11–13]. The comparison with our results on the most stable solids of the doped clusters shows that

Table 1. The binding (cohesive) energies (BE) in eV/atom for clusters and molecular solids formed from them, calculated with respect to the isolated atoms with the GGA and GGS levels of theory. The stabilization energies (SE) are shown. n_π is the number of π bonds per cluster and Δ stands for band or HOMO–LUMO gap in the GGA level of theory. The point or space group symmetry is given and the open or closed cluster configuration is indicated. The SEs are not affected by the values of the isolated atoms. corrections.

Compound	Lattice	Space group	BE(GGA) (eV)	BE(GGS) (eV)	SE(GGA) (eV)	n_π	Δ (eV)	ρ (g cm^{-3})
Graphite		$P6_3/mmc$	9.47	8.34	—	20	0	
Diamond		$Fd\bar{3}m$	9.32	8.19	—	0	4.68	
B_8C_{12}	Cluster	(T_h)	7.42	6.73	0.00	6	1.27	—
B_8C_{12}	sc (open)	$Pm\bar{3}$	7.93	7.24	10.06	6	0.00	2.072
B_8C_{12}	trc	$R\bar{3}$	7.89	7.20	9.42	6	0.00	2.687
B_8C_{12}	orc	$Immm$	7.73	6.90	6.20	6	0.00	2.111
B_8C_{12}	bcc	$C2/m$	7.56	6.68	2.80	6	0.00	1.481
B_8C_{12}	fcc	$Fm\bar{3}$	7.55	6.69	2.60	6	0.00	2.259
C_{20}	Cluster	(I_h)	8.30	7.17	0	20	0.78	—
C_{20}	fcc	$Fm\bar{3}$	8.71	7.58	8.20	6	2.64	2.822
C_{20}	sc (open)	$Pm\bar{3}$	8.66	7.53	7.20	20	0.00	2.524
C_{20}	bcc	$C2/m$	8.07	6.94	−4.60	—	0.00	1.612
B_8N_{12}	Cluster	(T_h)	8.01	6.47	0	6	3.32	—
B_8N_{12}	fcc	$Fm\bar{3}$	8.13	6.52	2.40	6	0.00	2.917
B_8N_{12}	sc (open)	$Pm\bar{3}$	8.09	6.55	1.60	6	0.00	2.609
B_8N_{12}	bcc	$C2/m$	7.81	6.14	−4.00	—	0.00	—
N_8B_{12}	Cluster	(T_h)	7.81	6.78	0	0	3.09	—
N_8B_{12}	sc (open)	$Pm\bar{3}$	7.81	6.78	0.00	0	0.00	2.198
N_8B_{12}	fcc	$Fm\bar{3}$	7.54	6.46	−5.40	—	0.00	—
N_8B_{12}	bcc	$C2/m$	7.39	6.36	−8.40	—	0.00	—
N_8C_{12}	Cluster	(T_h)	7.87	8.29	0	20	0.00	—
N_8C_{12}	sc (closed)	$Pm\bar{3}$	8.52	6.92	13.00	24	2.64	2.688
N_8C_{12}	sc (open)	$Pm\bar{3}$	8.40	6.80	10.60	20	0.00	2.934
N_8C_{12}	orc	$Im\bar{3}$	7.65	6.05	−4.40	—	0.00	—
N_8C_{12}	fcc	$Fm\bar{3}$	7.57	5.97	−6.00	—	0.00	—
Si_8C_{12}	Cluster	(C_{2v})	6.80	5.90	0	6	0.28	—
Si_8C_{12}	sc (C_{2v}) (closed)	$Pmmm$	7.28	6.38	9.60	6	0.00	2.504
Si_8C_{12}	Cluster	(T_h)	6.77	5.87	−0.60	—	0.24	—
Si_8C_{12}	fcc	$Fm\bar{3}$	7.38	6.48	11.60	6	1.08	2.629
Si_8C_{12}	sc (open)	$Pm\bar{3}$	7.23	6.33	8.60	6	0.00	2.515
SiB_7C_{12}	Cluster	(T_h/C_1)	7.34	6.50	0	6	0.59	—
SiB_7C_{12}	sc (closed)	$R3$	7.84	7.00	10.00	0	0.00	2.045
SiB_7C_{12}	sc (open)	$R3$	7.64	6.80	6.00	6	0.00	2.013
SiB_7C_{12}	fcc	$Fm\bar{3}$	ns					
SiN_7C_{12}	Cluster	(T_h/C_1)	7.79	6.28	0	17	0.52	—
SiN_7C_{12}	sc (open)	$R3$	8.30	6.79	10.20	17	0.00	2.925
SiN_7C_{12}	sc (closed)	$R3$	8.19	6.68	8.00	21	0.00	2.701
SiN_7C_{12}	fcc	$Fm\bar{3}$	ns					
BN_7C_{12}	Cluster	(T_h/C_1)	7.90	6.40	0	17	1.10	—
BN_7C_{12}	sc (closed)	$R3$	8.44	6.94	10.80	21	1.86	2.588
BN_7C_{12}	sc (open)	$R3$	8.36	6.86	9.20	17	0.43	2.821
NB_7C_{12}	Cluster	(T_h/C_1)	7.55	6.62	0	9	1.62	—
NB_7C_{12}	sc (closed)	$R3$	7.85	6.92	6.00	0	1.13	2.019
NB_7C_{12}	sc (open)	$R3$	7.35	6.41	−4.00	—	0	2.056

there are fundamental differences in the preferred structures for the pristine and the doped clusters. The fcc phase of C_{20} (fcc-C_{22}) is more stable than the sc phase by about 1 eV/cluster. In contrast, B_8C_{12} sc was strongly favoured, even with respect to the trc phase, while the fcc and bcc were much less stable, with stabilization energies per cluster of only 2.60 and 2.80 eV (GGA), which are not enough to guarantee high stability. The next structure in the ordering, the orc, had a stabilization energy of 6.20 eV/cluster. These energy differences may allow synthesizing several phases, or that there may exist pathways from one to the others. We note that the two dominant phases were the sc (10.06 eV/cluster) and trc (9.42 eV/cluster), close to an orc phase, but contrarily to C_{20} the fcc phase is not energetically stable.

B_8N_{12} (T_h) and N_8B_{12} (T_h) in the two fcc structures were unstable. The most stable phase found was B_8N_{12} (T_h) in an sc structure with a stabilization energy of 1.60 eV/cluster. This energy is not sufficient to grant a high degree of stability. This cannot exclude the possibility of the existence of molecular solids or liquids with weak inter-cluster interactions.

All of the phases considered for C_{20} and B_8C_{12} are conductors, except C_{20} fcc, which is a semiconductor. This is an indication that the B_8C_{12} solid is metallic, for most of the phases that it adopts. It is noted that the difference between sc, trc and orc phases is small (less than 0.1 eV/atom), suggesting that they can possibly all be fabricated. There is a great number of other metastable phases with the same stoichiometry that do not involve the T_h or other clusters. We have found two such structures. One is the orc phase in figure 1 and the other has $P3/mmm$ space group symmetry and a cohesive energy 0.2 eV/atom smaller than the cluster assembled sc structure. These two were bulk metals but their energies were not competitive with the B_8C_{12} (T_h) sc.

The Si_8C_{12} (C_{2v}) sc phase was found to be very stable, as was Si_8C_{12} (T_h) fcc. The latter was the most stable of the two and was based on the T_h symmetry cluster, which is less stable than C_{2v} [12]. It is a semiconductor with a moderate direct bandgap of $\simeq$1.08 eV.

The mixed heterofullerenes SiB_7C_{12} (T_h/C_1), SiN_7C_{12} (T_h/C_1) and their solid phases were investigated. The notation designates the point group symmetry of the cluster skeleton, T_h, while the cluster itself is C_1. We have found that the stabilization energies for the sc phases are high (10.00 eV/cluster and 10.20 eV/cluster for SiB_7C_{12} (T_h/C_1) sc and SiN_7C_{12} (T_h/C_1) sc (open) respectively). Both were metallic. All other structures found had smaller stabilization energies and were metals. It is then concluded that the mixed heterofullerenes can also assemble in stable solid phases.

The SiB_7C_{12} (T_h/C_1) and SiN_7C_{12} (T_h/C_1) clusters were themselves structures of high stability, corresponding to strongly bound clusters [12].

The BN_7C_{12} (T_h/C_1) clusters were very stable and their binding energies were closest to that of C_{20}. This structure is probably a magic cluster and showed, like the other mixed heterofullerenes, a strong propensity to form solid phases. The stabilization energy in the sc closed cage configuration was 10.80 eV/cluster, a semiconductor with 1.80 eV bandgap.

The NB_7C_{12} sc (closed) cluster phase was the only stable phase found for this cluster with a stabilization energy of 6 eV/cluster.

4. Geometries and bonding

Figure 1 shows the several most frequent structures for the solids. The cells are not primitive. The fcc structures were optimized with 88 atoms: 20-atom clusters, two interstitial carbons per cluster and no symmetry constraints. Some of the phases were not just energetically unfavourable but also not geometrically stable and relaxed to different atomic configurations of no particular stability. In these cases they were designated by 'ns'.

The bcc lattice contained 48 atoms per primitive cell, where eight atoms were carbon interstitials. These phases were not found to be the most stable in any case and constituted a tentative metastable arrangement of small density.

Table 2 shows the average bond lengths, Mulliken charges, bond overlaps and lattice parameters for the solid phases studied. The type of structure is indicated as are the group symmetries. The cells used have been fully optimized in every case.

We have seen in section 3 that the B_8C_{12} sc (open) lattice was the most stable. Its geometry was consistent with this, as the sc (open) lattice had the shortest average B–C and C=C ethylenic bond lengths. The corresponding overlaps were also the highest obtained for the B_8C_{12} series, along with the Mulliken population difference between species. This is an indication of the reinforcement of both the covalent and ionic bonding.

Although the C_{20} fcc structure was the most stable in the C_{20} series, this is not due to the reinforcement of the bonds. The stabilization of this solid results from strong sp^3 bonds between the clusters and the interstitial carbon atoms, along with the formation of six C=C ethylenic bonds.

The B_8N_{12} and N_8B_{12} clusters were not found to form highly stable solids. This, combined with the fact that these clusters possess high bonding energy is an indication that they do not tend to form strongly bound crystalline solids. Among the weakly stable phases they form, the B_8N_{12} sc phase was the one where the combined B–N and N–N bonding was shorter and the B–N bond overlap largest. The Mulliken populations were closest to the isolated cluster and there was a slight reinforcement of the ionic contribution to the bonding.

The fcc phases of SiB_7C_{12} (T_h) and SiN_7C_{12} (T_h) were not stable and our optimized structures resulted either in phases of different symmetries or in structures where the integrity of the cluster was no longer maintained. The sc phase either open or closed was found to be lowest in energy with respect to all other phases of these clusters. The small C–C bond lengths and the higher covalent character of the bonding are a strong indication that these should be the most stable configurations for the solids.

The solid resulting from the BN_7C_{12} (T_h/C_1) cluster assembly featured bond elongation of the C_2 ethylenic units, as well as all other bonds. However, the ionic character of the bonding, through the larger Mulliken charges, was reinforced, resulting in an overall lowering of the total energy. This solid phase was then stabilized by stronger ionic bonding, detrimentally to the covalent character. The sc open configuration showed the opposite trend and the covalent character was reinforced.

The NB_7C_{12} sc structure showed a slight enhancement of the Mulliken charges and an overall increase of the N–C bonds. The C–C bonds were elongated, due to the inter-cluster bonding. The inter-cluster bonds ($\approx$1.54 Å) were shorter than the intra-cluster ones ($\approx$1.65 Å), indicating the favouring of the solid structure. The C–C overlap was correspondingly smaller.

As a general remark, valid for all structures but the ones involving elements with more valence electrons than carbon, the simple cubic closed cage structure has more bonds than the open cage configurations and this implies an electronic redistribution of the valence electrons from the clusters into a larger number of inter-cluster bonds. As a consequence, the number of π bonds is in every case smaller in the solid phase than in the isolated cluster. In most cases the C=C ethylenic bonds disappear in the solid phase and the number of weak secondary bonds becomes either very small or non-existent (SiB_7C_{12} sc (closed)).

5. Electronic structure

The electronic structures of the most stable solids were analysed and we tried to establish structure–property relationships. The least stable structures, since they are not probable, were

Table 2. The lattice type and cell parameters are indicated for the clusters. The bond lengths were taken as the averages between the atoms involved in the indicated type of bond and the same for bond overlaps. 'ns' stands for non geometrically stable configuration. The anti-bonding interactions are not shown.

			Cell parameters						Bond length (Å)			Bond overlap (e)			Charge (e)		
Compound	Lattice	Symmetry	a	b	c	α	β	γ	Y–C	X–C	C–C	Y–C	X–C	C–C	X	C	Y
Graphite		$P6_3/mmc$	2.44	2.44	7.14	90	90	120	—	—	1.41	—	—	5.62	—	0.00	—
Diamond		$Fd\bar{3}m$	3.54	3.54	3.54	90	90	90	—	—	1.53	—	—	0.75	—	0.00	—
B_8C_{12}	Cluster	(T_h)	—	—	—	—	—	—	—	1.57	1.38	—	0.88	1.15	0.53	−0.35	—
B_8C_{12}	sc (open)	$Pm\bar{3}$	5.70	5.70	5.70	90.00	90.00	90.00	—	1.55	1.37	—	0.95	1.29	0.50	−0.33	—
B_8C_{12}	trc	$R\bar{3}$	5.69	5.70	5.70	83.53	96.59	83.36	—	1.56	1.38	—	0.90	1.23	0.44	−0.30	—
B_8C_{12}	orc	$Immm$	5.69	5.69	5.69	122.94	90.49	116.59	—	1.68	1.48	—	0.66	0.90	0.35	−0.23	—
B_8C_{12}	bcc	$C2/m$	8.56	8.54	8.55	89.97	90.00	90.00	—	1.60	1.33	—	0.78	1.46	0.37	−0.18	—
B_8C_{12}	fcc	$Fm\bar{3}$	9.12	8.97	9.15	88.89	88.81	89.59	—	1.64	1.29	—	0.74	1.56	0.43	−0.18	—
C_{20}	Cluster	(I_h)	—	—	—	—	—	—	—	—	1.44	—	—	1.02	—	0.00	—
C_{20}	fcc	$Fm\bar{3}$	8.58	8.44	8.58	89.99	89.99	89.98	—	—	1.49	—	—	0.93	—	0.00	—
C_{20}	sc (open)	$Pm\bar{3}$	5.41	5.41	5.41	90.00	90.00	90.00	—	—	1.43	—	—	1.05	—	0.00	—
C_{20}	bcc	$C2/m$	8.41	8.44	8.37	89.92	90.00	90.00	—	—	1.49	—	—	0.92	—	0.00	—
B_8N_{12}	Cluster	(T_h)	—	—	—	—	—	—	—	1.45	1.51	—	0.87	0.49	0.85	−0.56	—
B_8N_{12}	sc	$Pm\bar{3}$	5.45	5.45	5.45	90.00	89.98	90.00	—	1.45	1.43	—	0.91	0.59	0.76	−0.51	—
B_8N_{12}	bcc	$C2/m$	6.64	8.12	9.07	94.30	90.00	90.00	—	1.54	1.37	—	0.70	0.75	0.73	−0.37	—
B_8N_{12}	fcc	$Fm\bar{3}$	8.68	8.52	8.70	88.90	89.81	89.59	—	1.37	1.54	—	0.75	0.70	0.73	−0.37	—
N_8B_{12}	Cluster	(T_h)	—	—	—	—	—	—	—	1.46	1.68	—	0.81	0.96	0.51	−0.76	—
N_8B_{12}	sc	$Pm\bar{3}$	5.67	5.68	5.67	89.91	90.07	90.09	—	1.46	1.67	—	0.84	0.92	0.48	−0.72	—
N_8B_{12}	bcc	$C2/m$	6.64	8.12	9.07	94.30	90.00	90.00	—	1.54	1.29	—	0.67	0.92	0.82	−0.41	—
N_8B_{12}	fcc	$Fm\bar{3}$	8.68	8.52	8.70	88.90	89.81	89.59	—	1.54	1.37	—	0.70	0.75	0.73	−0.37	—
N_8C_{12}	Cluster	(T_h)	—	—	—	—	—	—	—	1.44	1.39	—	0.68	1.17	−0.31	0.20	—
N_8C_{12}	sc	$Pm\bar{3}$	5.42	5.41	5.42	90.00	90.00	90.00	—	1.46	1.56	—	0.75	0.69	−0.36	0.24	—
N_8C_{12}	sc (open)	$Pm\bar{3}$	5.25	5.26	5.25	89.96	89.98	90.06	—	1.42	1.36	—	0.83	1.37	−0.34	0.23	—
N_8C_{12}	orc	$Im\bar{3}$	5.73	5.73	5.73	109.41	109.41	109.58	—	1.48	1.45	—	0.71	0.99	−0.17	0.11	—
N_8C_{12}	fcc	$Fm\bar{3}$	8.36	8.21	8.39	88.90	89.81	89.59	—	1.51	1.43	—	0.63	1.10	−0.18	0.10	—

Table 2. (Continued.)

			Cell parameters						Bond length (Å)			Bond overlap (e)			Charge (e)		
Compound	Lattice	Symmetry	*a*	*b*	*c*	α	β	γ	Y–C	X–C	C–C	Y–C	X–C	C–C	X	C	Y
Si_8C_{12}	Cluster	(C_{2v})	—	—	—	—	—	—	—	1.87	1.35	—	0.68	1.24	1.05	−0.70	—
Si_8C_{12}	sc (C_{2v})	*Pmmm*	6.61	7.48	4.95	90.11	89.95	90.02	—	1.88	1.55	—	0.65	0.67	0.90	−0.60	—
Si_8C_{12}	Cluster	(T_h)	—	—	—	—	—	—	—	1.85	1.37	—	0.79	1.16	1.08	−0.72	—
Si_8C_{12}	sc (open)	*Pmmm*	6.55	5.75	6.47	90.03	89.97	89.97	—	1.94	1.36	—	0.67	1.30	1.03	−0.69	—
Si_8C_{12}	fcc (T_h)	$Fm\bar{3}$	7.11	7.10	7.05	57.98	60.01	59.06	—	1.81	1.36	—	0.76	1.26	1.44	−0.82	—
SiB_7C_{12}	Cluster	(T_h/C_1)	—	—	—	—	—	—	1.87	1.60	1.38	0.71	0.87	1.15	0.52	−0.39	1.05
SiB_7C_{12}	sc	*R*3	5.87	5.86	5.86	91.24	88.69	88.71	1.88	1.57	1.58	0.63	0.91	0.61	0.53	−0.39	0.96
SiB_7C_{12}	sc (open)	*R*3	5.78	5.78	5.78	90.59	89.95	90.30	1.80	1.56	1.37	0.81	0.95	1.30	0.47	−0.38	1.34
SiB_7C_{12}	fcc	$Fm\bar{3}$	ns														
SiN_7C_{12}	Cluster	(T_h/C_1)	—	—	—	—	—	—	1.92	1.45	1.34	0.52	0.73	1.31	−0.33	0.13	0.78
SiN_7C_{12}	sc (open)	*R*3	5.50	5.50	5.50	92.13	87.78	87.74	1.82	1.43	1.36	0.80	0.69	1.34	−0.39	0.09	1.27
SiN_7C_{12}	sc	*R*3	5.36	5.35	5.36	91.37	91.26	91.47	1.89	1.46	1.56	0.54	0.75	0.69	−0.36	0.13	0.99
SiN_7C_{12}	fcc	$Fm\bar{3}$	ns														
BN_7C_{12}	Cluster	(T_h/C_1)	—	—	—	—	—	—	1.52	1.46	1.34	0.92	0.73	1.30	−0.34	0.15	0.50
BN_7C_{12}	sc	*R*3	5.46	5.46	5.46	90.98	88.98	88.98	1.54	1.46	1.54	0.85	0.75	0.70	−0.36	0.16	0.65
BN_7C_{12}	sc (open)	*R*3	5.30	5.30	5.30	90.69	90.58	90.61	1.54	1.43	1.36	0.93	0.82	1.37	−0.34	0.15	0.54
NB_7C_{12}	Cluster	(T_h/C_1)	—	—	—	—	—	—	1.44	1.56	1.38	0.80	0.88	1.15	0.53	−0.30	−0.28
NB_7C_{12}	sc	*R*3	5.77	5.77	5.77	89.76	90.51	90.38	1.49	1.58	1.54	0.74	0.83	0.66	0.56	−0.30	−0.35
NB_7C_{12}	sc (open)	*R*3	5.74	5.74	5.74	90.86	90.22	90.14	1.45	1.58	1.38	0.79	0.94	1.29	0.49	−0.27	−0.28

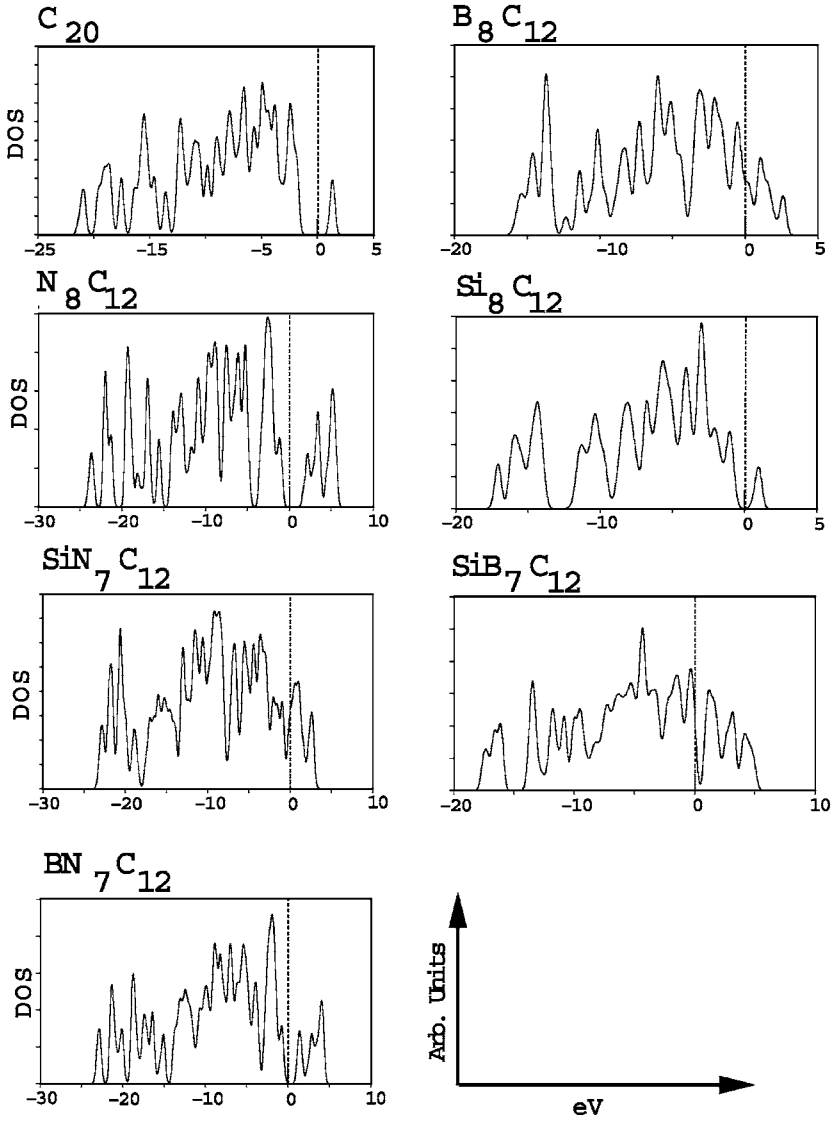

Figure 2. The DOS for the most stable solids (C_{20} fcc, B_8C_{12} sc (closed), N_8C_{12} sc (closed), Si_8C_{12} fcc, SiN_7C_{12} sc (open), SiB_7C_{12} sc (closed) and BN_7C_{12} sc (closed)). B_8C_{12} sc (open) and SiB_7C_{12} sc (closed) are possible candidates to exhibit high T_c superconductivity, displaying a large DOS at the Fermi level of dominant p-type orbitals.

not analysed in detail. Also, the k-space directions were chosen with respect to the supercells and not the primitive lattices, resulting in a denser k-point set, sometimes complemented by extra points without special symmetry.

5.1. Density of states and band structures

The density of states and band structures for the most stable solids are shown in figures 2 and 3. The dominant contribution at the Fermi level is p for all conductors.

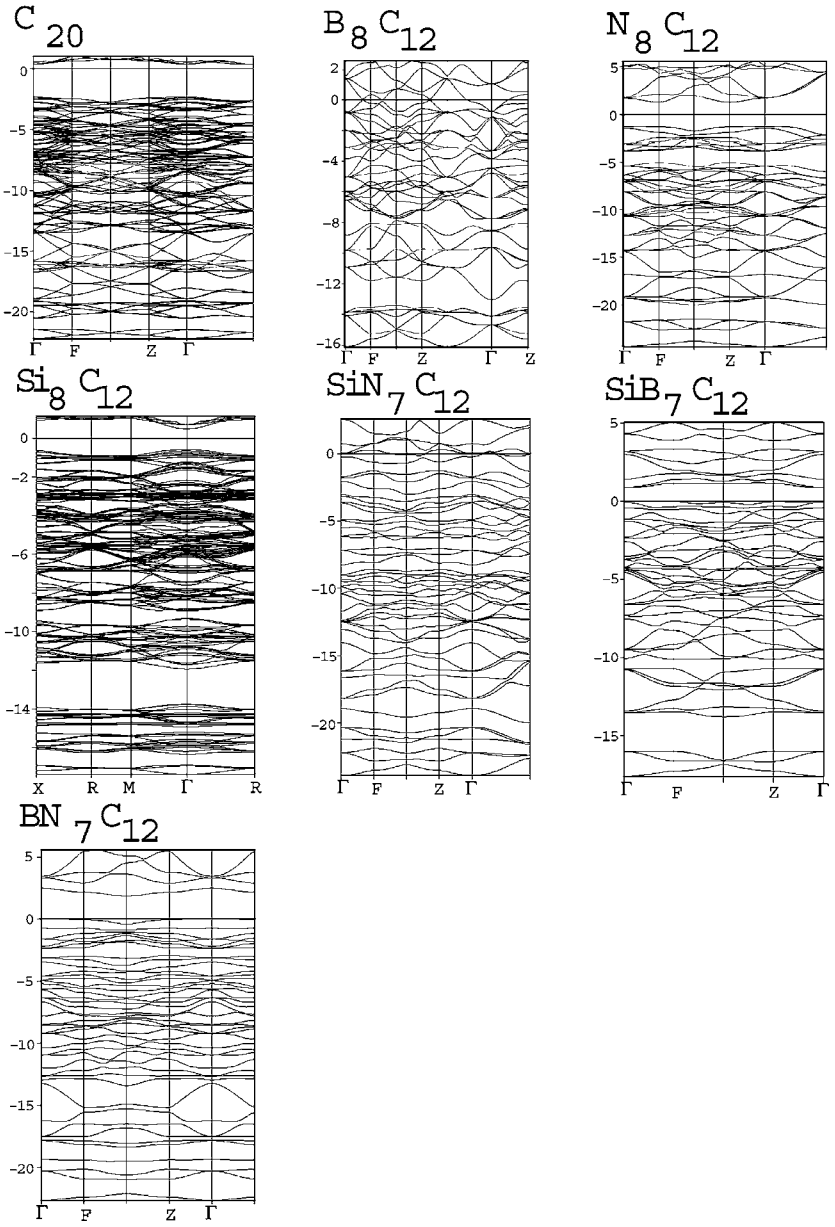

Figure 3. The band structures (in eV) associated with the DOS in figure 1. We can see the position of the Fermi level for SiB_7C_{12} and BN_7C_{12} located at the top of the valence band. Si_8C_{12} and B_8C_{12} are metals and the rest are moderate bandgap semiconductors. Si_8C_{12} has a direct bandgap.

The C_{20} fcc solid (fcc-C_{22}) is a semiconductor. The large DOS feature at the valence band edge (≈34.8 electrons/eV) can possibly be used for low resistivity conduction through hole-injection [11]. The band structure shows that the material has a ΓR bandgap of 2.64 eV and this value is in reasonable agreement with Spagnolatti *et al* [11] with a reported XL gap of 2.47 eV (this author did not considered the R point). The difference is attributed to the type

of pseudopotential used and to the fact that we have considered more symmetry points. We have obtained an XL bandgap of 2.80 eV, consistent with the trend toward larger bandgaps produced by ultrasoft pseudo-potentials.

B_8C_{12} sc is a bulk metal. The DOS shows a value that is relatively low at the Fermi level (3.5 electrons/eV) and no peak can be seen. The band structure shows no distinctive features other than band crossings at the Fermi level.

N_8C_{12} sc is a semiconductor with a moderate indirect bandgap (2.64 eV FZ).

The Si_8C_{12} (T_h) fcc phase is a semiconductor with a moderate direct bandgap of 1.08 eV. The DOS shows a peak at the valence band edge that, like in C_{20} fcc, can be tuned through carrier doping.

SiN_7C_{12} sc (open) is a conductor with a peak of the DOS (4.3 electrons/eV) at the Fermi level. This is a noticeable feature, suggesting that the material may show superconductivity. The closed cage crystal structure is also a metal with a DOS peak at the Fermi level. Like B_8C_{12} the various most stable structures have the same conductive character.

SiB_7C_{12} displays a DOS peak (5 electrons/eV) at the Fermi level of dominant p type. The material is thus a conductor and a high T_c superconductor candidate. The DOS suggests that hole conduction is probable. The band structure shows that the peak at the chemical potential results from a single band at the valence band edge with $\approx$0.22 eV dispersion. The band gap is FG, with a value of 0.97 eV.

BN_7C_{12} sc (closed) displays a DOS peak below the Fermi level ($\approx$4.43 electrons/eV). The material is a semiconductor with a bandgap of 2.30 eV. The band structure shows that the peak results from a single band with a dispersion 0.4 eV near the top of valence band.

NB_7C_{12} sc (closed) is a semiconductor with a multiple direct bandgap of 1.13 eV (at the Z and F points) and a peak at the top of the valence band. This material may become a superconductor under hole-doping conditions.

All the mixed clusters exhibited a peak of the DOS at or immediately below the chemical potential, originating mostly from a single band, with NB_7C_{12} and SiB_7C_{12} being the most pronounced.

5.2. Conductors and superconductivity

The number of π bonds in these systems is inversely proportional to the electron–phonon coupling parameter λ [10]. The number of π bonds in C_{20} is 20, as the system is π conjugated, and the e–ph coupling is known to be strong. In other related clusters this number can be lower but not higher. In particular the B_8C_{12} clusters have only six π bonds and others involving N and Si are intermediate. Therefore, all the clusters studied have between zero and 20 π bonds, showing that it is, in principle, possible to produce an arbitrary number of such bonds in carbon based crystalline solids. When in a solid phase the number of bonds, in all but the sc (open) lattice, increases and electrons are called to participate in inter-cluster σ bonding. Then the number of π bonds in the solids is systematically lowered relative to the isolated clusters and hence an improvement of the coupling parameters becomes a trend, according to this criterion. On the other hand, the lighter elements involved in the boron–carbon clusters provide another indication of the enhancement of e–ph coupling. All the cluster phases which are metallic, have a small number of π bonds, a high level of crystallinity and involve light elements meet the primary requirements. Also, SiB_7C_{12} has a larger DOS peak at the Fermi level resulting from p-type contributions and the small dispersion of the band that produces the peak suggests that single-band conduction may be possible. All the above criteria point to enhanced coupling and superconductivity. The best candidates that we have found are in order SiB_7C_{12}, B_8C_{12} and SiN_7C_{12}.

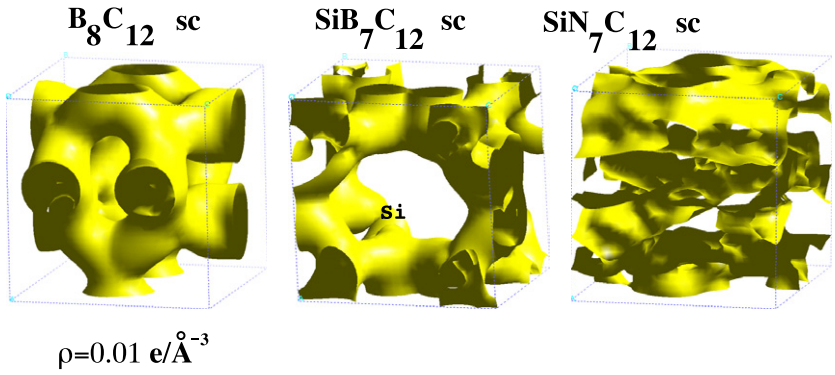

Figure 4. The charge densities at the Fermi energy. The SiB_7C_{12} and B_8C_{12} clusters have a continuous 2D conductive surface, while BN_7C_{12} does not. The position of the Si atom is shown and this surface results from a single band.

(This figure is in colour only in the electronic version)

The variety of mixed element clusters that can be envisaged, with the general propensity to nucleate solid phases establishes the potential for modulation and design of a large number of high T_c superconducting polymers through cluster assembly, that have low density and are crystalline. The mixing of not only different elements in the clusters but also of different cluster combinations adds to the variety of solids that can be construed.

Figure 4 shows the electron density at the Fermi level in real space for the most stable metals (0.01 electrons/$Å^{-3}$). We note that the surfaces of B_8C_{12} sc (open) and SiB_7C_{12} sc (closed) form a network of conducting channels that are nearly isotropic and two dimensional. The SiB_7C_{12} sc (closed) surface results from a single band with a dispersion of 0.22 eV. The SiN_7C_{12} sc (open) charge density surface is delocalized and does not show a 2D conductive surface.

Some of the semiconductors found had a large direct bandgap. The semiconductors which had both a large stabilization energy and large bandgaps were N_8C_{12} sc (closed), C_{20} fcc and BN_7C_{12} sc (closed). These materials may find uses in optical applications.

6. Conclusions

We have confirmed the high stability of the solid phases of B_8C_{12} (T_h) sc (open), C_{20} fcc and N_8C_{12} (T_h) sc (closed), SiB_7C_{12} (T_h) sc (closed), SiN_7C_{12} (T_h) sc (open), SiB_7C_{12}, BN_7C_{12} and NB_7C_{12}, showing for the first time that molecular solids of these clusters are possible. The improbable existence of solid phases of the clusters B_8N_{12} (T_h) and N_8B_{12} (T_h) was suggested and the existence of five new solids of high stability is proposed (two conductors and three semiconductors); SiB_7C_{12} (T_h) sc, SiN_7C_{12} (T_h) sc (open), BN_7C_{12}, NB_7C_{12} and Si_8C_{12} fcc have all shown high stabilization energies. The SiN_7C_{12}, B_8C_{12} and SiB_7C_{12} most stable phases were metallic and show potential for strong electron–phonon coupling and high T_c superconductive behaviour. SiB_7C_{12} and SiN_7C_{12} had a peak of the DOS at the Fermi level, which is an improvement over undoped C_{20} fcc. In particular, SiB_7C_{12} with a small number of π bonds shows all the traits necessary to enhance the effect, including a single small dispersion band for conduction, a higher value of DOS at the Fermi level (5 electrons/eV), a large number of light elements and a 2D connected, conductive electronic isodensity surface.

We have also calculated the bandgaps of the semiconductors and found that there are new ones with potentially novel applications. N_8C_{12} sc (closed), C_{20} fcc and BN_7C_{12} sc (closed) all

have large bandgaps. Si_8C_{12} (T_h/C_1) in an fcc lattice is a highly stable semiconducting phase with a direct bandgap of 1.08 eV. The mixed clusters have unpaired spins and their associated solids may have novel dielectric or magnetic characteristics.

This work demonstrates the potential for the design of high T_c superconductors and novel semiconductors through cluster assembly of C_{20} and associated heterofullerenes. In particular, the number of π bonds can be manipulated and we have illustrated how to obtain organic covalent solids with a variable number of such bonds.

Acknowledgments

HSD acknowledges PRAXIS XXI/BD/13944/97. Some of the calculations were carried out at the Cambridge-Cranfield HPCF, England. Thanks are due to Dr C-K Skylaris for help with the revision of the manuscript and help with figure 1, and to Dr P Hasnip for technical support.

References

[1] Guo B C, Kerns K P and Castleman A W Jr 1992 *Science* **255** 1411
[2] Rohmer M-M, Benard M and Poblet J M 2000 *Chem. Rev.* **100** 495
[3] Prinzbach H *et al* 2000 *Nature* **407** 60
[4] Yang C *et al* 1996 *Acta Chim. Sin.* **54** 1041
[5] Alder R W, Harvey J N, Schleyer P V and Moran D 2001 *Org. Lett.* **3** 3233
[6] Bode B M and Gordon M S 1999 *J. Chem. Phys.* **11** 8778
[7] Evangelisti S 1997 *Int. J. Quantum Chem.* **65** 83
[8] Domingos H S and Bristowe P D 2005 *J. Clust. Sci.* submitted
[9] Iqbal Z *et al* 2003 *Eur. Phys. J.* B **31** 509
[10] Devos A and Lanoo M 1998 *Phys. Rev.* B **58** 8236
[11] Spagnolatti I, Bernasconi M and Benedek G 2002 *Europhys. Lett.* **59** 572
[12] Domingos H S and Bristowe P D 2003 *J. Phys.: Condens. Matter* **15** 4341
[13] Saito M, Miyamoto Y and Okada S 2002 *Mol. Cryst. Liq. Cryst.* **386** 97
[14] Saito M and Miyamoto Y 2001 *Phys. Rev. Lett.* **87** 35503
[15] Miyamoto Y and Saito M 2001 *Phys. Rev.* B **63** 161401
[16] Okada S, Miyamoto Y and Saito M 2001 *Phys. Rev.* B **64** 245405
[17] Gao L, Lyn M E, Bergeron D E and Castleman A W 2003 *Int. J. Mass Spectrom.* **229** 11
[18] Baruah T and Pederson M R 2002 *Phys. Rev.* B **66** 241404
[19] Chen Z F *et al* 2004 *J. Phys. Org. Chem.* **16** 726
[20] Perdew J *et al* 1992 *Phys. Rev.* B **46** 6671
[21] *Cerius*^{2} *User Guide MSI/Accelrys* 1999
[22] Vanderbilt D 1990 *Phys. Rev.* B **41** 7892
Laasonen K *et al* 1993 *Phys. Rev.* B **47** 10142
[23] Monkhorst H J and Pack J D 1976 *Phys. Rev.* B **13** 5188
[24] Segall M D, Pickard C J, Shah R and Payne M C 1996 *Mol. Phys.* **2** 16317